Theoret.Appl.Mech. TEOPM7, Vol.41,No.1,pp.71–91, Belgrade 2014*

UNSTEADY FLOW OF A MICROPOLAR FLUID GENERATED BY A CIRCULAR CYLINDER SUBJECT TO LONGITUDINAL AND TORSIONAL OSCILLATIONS

G.Nagaraju J.V.Ramana Murthy

*doi:10.2298/TAM1401071N Math. Subj. Class.: 74A35; 74A60; 76A99.

According to: *Tib Journal Abbreviations (C) Mathematical Reviews*, the abbreviation TEOPM7 stands for TEORIJSKA I PRIMENJENA MEHANIKA.

Theoret. Appl. Mech., Vol.41, No.1, pp. 71–91, Belgrade 2014

Unsteady flow of a micropolar fluid generated by a circular cylinder subject to longitudinal and torsional oscillations

G.Nagaraju * **J.V.Ramana Murthy**†

Abstract

The flow generated by a circular cylinder, performing longitudinal and torsional oscillations, in an infinite expanse of a micropolar fluid is studied. Analytical expressions for the velocity and micro rotation components are obtained using no slip and hyper stick conditions at the boundaries. The effects of coupling number, Reynolds number and gyration parameter on the transverse and axial velocity components are shown and explained graphically. Also explicit expression for the drag force acting on the wall of the cylinder is derived and the effects of pertinent parameters on the drag are shown graphically.

Keywords: Micropolar fluid; circular cylinder; coupling number; longitudinal and torsional oscillations; drag.

1 Introduction

Mathematical description of micropolar fluid was introduced by Eringen [1] in 1966 as a special case of polar fluids. A micropolar fluid is a non-Newtonian fluid with local microstructure exhibiting micro rotations. The theory of micropolar fluids can be applied in many situations where fluids like lubricating fluids, dusty fluids and additives, certain polymer solutions, colloidal suspensions and complex biological fluid structures etc. are involved. The flow of a fluid due to a cylindrical rod oscillating with longitudinal and torsional motion has received considerable attention because of its relevance in many

*Department of Mathematics, Gitam University, Hyderabad, Rudraram, Medak Dist(A.P), 506004, India

†NIT Warangal (A.P),506004,India

technical problems of practical importance such as mixing, oil drilling and towing operations.

The motion of a classical viscous fluid due to the rotation of an infinite cylindrical rod immersed in the fluid was first described by Stokes [3]. External flows generated due to longitudinal and torsional oscillations of a rod were found in the classical papers of Casarella, Laura [4]. Rajagopal [5] studied the same problem for the case of a second grade fluid. The motion of a classical viscous fluid inside an infinite cylinder was studied by Ramkissoon [6] and he derived an analytical expression for shear stresses, drag on the cylinder and velocity was depicted graphically. Camlet-Eluhu, Majumdar [7] have investigated the same problem for a micropolar fluid and examined the effect of micropolar fluid on the two components of the velocity field through graphical curves by using Mathematica. Owen and Rahman [8] studied the same type of flow with an Oldroyd-B liquid. Calmelet-Eluhu, Rosenhaus [9] studied, micropolar fluid inside a moving infinite circular cylinder due to its oscillations along and about its axis and they found analytical solutions by applying lie group methods. Using various types of fluids, the flow generated due to longitudinal and torsional oscillations of a circular cylinder was examined by few authors. Ramkissoon et al [10] have examined a polar fluid by using transform methods and they have presented the effect of micropolar parameters on the microrotation and velocity fields graphically. Bandelli et al [11] studied the flow of third grade fluid. Rajagopal and Bhatnagar [12] presented two simple but elegant solutions for the flow of an Oldroyd-B fluid. In the first part, they considered the flow past an infinite porous plate and found that the problem admits an automatically decaying solution in the case of suction at the plate and that in the case of blowing it admits no such solution. In the second part, they studied longitudinal and torsional oscillations of an infinitely long rod of finite radius. Pontrelli [13] has studied the axi-symmetric flow of a homogeneous Oldroyd-B fluid with suction or injection velocity applied at the surface. Akyildiz [14] studied an Oldroyd-B fluid and he examined the effect of the elasticity on the velocity field and dynamic boundary layer. Fatacau and Corina Fatacau [15] have obtained the starting solutions corresponding to the motion of a second grade fluid by means of the finite Hankel transforms. Vieru et al[16] investigated the exact solutions for the motion of a Maxwell fluid using Laplace Transforms. Karim Rahaman et al[17] studied the motion of viscoelastic incompressible flow of the upper convected Maxwell fluid at different frequencies of oscillations of the cylinder along and about its axis and he presented velocity components graphically for particular values of the flow parameters. Mehrdad Massoudi and Tran

X.Phouc [18] have solved numerically the flow of a second grade fluid and they presented the results graphically for the shear stresses at the wall. But not much literatures is available on the flow due to oscillations of a rod in micropolar fluids. Hence, in this paper we consider the flow of micropolar fluid generated by a circular cylinder subjected to longitudinal and torsional oscillations.

2 Description and formation of the problem

Consider a circular cylinder of radius 'a' within an incompressible micropolar fluid. The cylinder is subjected to torsional oscillations $e^{i\omega_1\tau}$ and longitudinal oscillations $e^{i\omega_2\tau}$ with amplitudes $q_0 sin\beta_0$, $q_0 cos\beta_0$ along the respective directions with ω_1 as the frequency of the torsional oscillations, ω_2 as the frequency of the longitudinal oscillations, q_0 as the magnitude of oscillations and β_0 is the angle between the direction of torsional oscillation and the base vector $\mathbf{e}_\theta$. i.e the cylinder oscillates with velocity as given by the expression $Q_\Gamma = q_0 \left(\mathrm{Sin}\beta_0 e^{i\omega_1\tau} e_\theta + \mathrm{Cos}\beta_0 e^{i\omega_2\tau} e_z \right)$ and the flow of the micropolar fluid being generated due to these oscillations of the cylinder. Choose the cylindrical polar coordinate system (R,θ, Z) with the origin at the center of the cylinder and Z-axis along the axis of the cylinder. The physical model illustrating the problem under consideration is shown in figure 1.

After neglecting body forces and body couples, the field equations governing the incompressible micropolar fluid dynamics as proposed by Eringen [1] are

$$\nabla_1 \cdot Q = 0 \tag{1}$$

$$\rho\left(\frac{\partial Q}{\partial \tau} + Q.\nabla_1 Q\right) = -\nabla_1 P + \kappa\nabla_1 \times l - (\mu+\kappa)\,\nabla_1 \times \nabla_1 \times Q \tag{2}$$

$$\rho j\left(\frac{\partial l}{\partial \tau} + Q\cdot\nabla_1 l\right) = -2\kappa l + \kappa\nabla_1 \times Q - \gamma\nabla_1 \times \nabla_1 \times l + (\alpha+\beta+\gamma)\,\nabla_1\left(\nabla_1 \cdot l\right) \tag{3}$$

where Q is velocity, P is Pressure, l is micro-rotation vector,j is micro-inertia coefficient, ρ is density, τ is time, The constants α,β, γ, κ and μ are material coefficients which satisfy the following inequalities

$$2\mu+\kappa \geq 0 \quad \kappa \geq 0 \quad 3\alpha+\beta+\gamma \geq 0 \quad \gamma \geq |\beta|$$

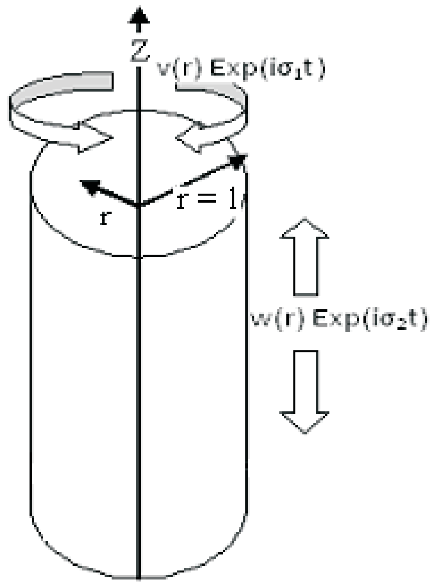

Figure 1: Geometry of the problem–non dimensional form

By nature of the geometry and flow, the velocity and micro-rotation components are assumed to be axially symmetric and depend only on radial distance and time. Hence the velocity and micro-rotations are taken in the form

$$Q = V(R,\tau)\, e_\theta + W(R,\tau)\, e_z \tag{4}$$

$$l = B(R,\tau)\, e_\theta + C(R,\tau)\, e_z \tag{5}$$

By introducing the following non-dimensional scheme

$$q = \frac{Q}{q_0}, \quad \upsilon = \frac{a}{q_0} l, \quad p = \frac{P}{\rho q_0^2}, \quad t = \frac{q_0}{a}\tau, \quad r = \frac{R}{a} \ \ and \ \ z = \frac{Z}{a} \tag{6}$$

The equations in (1), (2) and (3), for the flow take the following non-dimensional form

$$\nabla \cdot q = 0 \tag{7}$$

$$Re\left(\frac{\partial q}{\partial t} + q.\nabla q\right) = -Re\nabla p + c\nabla \times \upsilon - \nabla \times \nabla \times q \tag{8}$$

$$\varepsilon\left(\frac{\partial \upsilon}{\partial t} + q.\nabla \upsilon\right) = -2s\upsilon + s\nabla \times q - \nabla \times \nabla \times \upsilon \tag{9}$$

where cross viscosity parameter (also known as coupling number) c, couple stress parameter s, Reynolds number Re and gyration parameter ε are given by

$$c = \frac{\kappa}{\kappa + \mu}, \quad s = \frac{\kappa a^2}{\gamma}, \qquad Re = \frac{\rho q_0 a}{\mu + \kappa} \quad \textit{and} \;\; \varepsilon = \frac{\rho j q_0 a}{\gamma} \tag{10}$$

Let us choose the velocity vector $\boldsymbol{q}$ and micro-rotation vector υ in the form

$$q = v\,(r)\, e^{i\sigma_1 t} e_\theta + w\,(r)\, e^{i\sigma_2 t} e_z \tag{11}$$

$$\upsilon = B\,(r)\, e^{i\sigma_2 t} e_\theta + C\,(r)\, e^{i\sigma_1 t} e_z \tag{12}$$

$$p = p_1\,(r)\, e^{2i\sigma_1 t} \tag{13}$$

where $\sigma_1 = \dfrac{\omega_1 a}{q_0}$ and $\sigma_2 = \dfrac{\omega_2 a}{q_0}$

Substituting (11)–(13) in (8) and comparing the coefficients of $\boldsymbol{e}_r, \boldsymbol{e}_\theta,\ \boldsymbol{e}_z$ we get

$$\frac{dp_1}{dr} = \frac{v^2}{r} \tag{14}$$

$$Rei\sigma_1 v = -c\frac{dC}{dr} + \frac{d^2 v}{dr^2} + \frac{1}{r}\frac{dv}{dr} - \frac{v}{r^2} \tag{15}$$

$$Rei\sigma_2 w = c\left(\frac{dB}{dr} + \frac{B}{r}\right) + \left(\frac{d^2 w}{dr^2} + \frac{1}{r}\frac{dw}{dr}\right) \tag{16}$$

Similarly the equation (9) yields the following equations

$$\varepsilon\frac{Bv}{r} e^{i(\sigma_1+\sigma_2)t} = 0 \tag{17}$$

$$\varepsilon i\sigma_2 B = -2sB - s\frac{dw}{dr} + \frac{d^2 B}{dr^2} + \frac{1}{r}\frac{dB}{dr} - \frac{B}{r^2} \tag{18}$$

$$\varepsilon i\sigma_1 C = -2sC + s\left(\frac{dv}{dr} + \frac{v}{r}\right) + \left(\frac{d^2 C}{dr^2} + \frac{1}{r}\frac{dC}{dr}\right) \tag{19}$$

Eliminating $\dfrac{dC}{dr}$ from (15) and (19) we get

$$\left[D^4 - (i\sigma_1\,(Re+\varepsilon) + s\,(2-c))\, D^2 + iRe\sigma_1\,(i\varepsilon\sigma_1 + 2s)\right] v = 0 \tag{20}$$

where $D^2 = \dfrac{d^2}{dr^2} + \dfrac{1}{r}\dfrac{d}{dr} - \dfrac{1}{r^2}$

This can be written as

$$\left(D^2 - \lambda_1^2\right)\left(D^2 - \lambda_2^2\right) v = 0 \tag{21}$$

where $\lambda_1^2+\lambda_2^2 = i\sigma_1\left(Re+\varepsilon\right)+s\left(2-c\right)$ and $\lambda_1^2\lambda_2^2 = iRe\sigma_1\left(i\varepsilon\sigma_1+2s\right)$

Similarly equation (16) and (18) reduces to

$$\left[D^4-\left(i\sigma_2\left(Re+\varepsilon\right)+s\left(2-c\right)\right)D^2+iRe\sigma_2\left(i\varepsilon\sigma_2+2s\right)\right]B=0 \qquad (22)$$

which can be written as

$$\left(D^2-\alpha_1^2\right)\left(D^2-\alpha_2^2\right)B=0 \qquad (23)$$

where $\alpha_1^2+\alpha_2^2 = i\sigma_2\left(Re+\varepsilon\right)+s\left(2-c\right)$ and $\alpha_1^2\alpha_2^2 = iRe\sigma_2\left(i\varepsilon\sigma_2+2s\right)$

From equation (15) we notice that

$$\frac{dC}{dr}=\frac{1}{c}\left(D^2-iRe\sigma_1\right)v \qquad (24)$$

Substituting the expression (24) for $\frac{dC}{dr}$ in (19) we may obtain the equation for C as

$$c\left(i\sigma_1\varepsilon+2s\right)C = v''' + \frac{2}{r}v'' + \left(b_1-\frac{1}{r^2}\right)v' + \left(\frac{b_1}{r}+\frac{1}{r^3}\right)v \qquad (25)$$

Similarly from equation (18), we have

$$\frac{dw}{dr}=\frac{1}{s}\left(D^2-2s-i\sigma_2\varepsilon\right)B \qquad (26)$$

Substituting the expression (26) for $\frac{\partial w}{\partial r}$ in (16) we obtain the equation for w as

$$isRe\sigma_2 w = B''' + \frac{2}{r}B'' + \left(b_2-\frac{1}{r^2}\right)B' + \left(\frac{b_2}{r}+\frac{1}{r^3}\right)B \qquad (27)$$

Now the equations (21) and (23) are solved for v and B under the no slip and hyper stick conditions.

No slip condition: Velocity on the boundary equals to

$$\mathbf{Q}_\Gamma = \mathbf{q}_0\left(cos\beta_0 e^{i\omega_1\tau}\mathbf{e}_\theta + sin\beta_0 e^{i\omega_2\tau}\mathbf{e}_z\right)$$

which in non–dimensional form is given by $\mathbf{q}|_{r=1} = cos\beta_0 e^{i\sigma_1 t}\mathbf{e}_\theta + sin\beta_0 e^{i\sigma_2 t}\mathbf{e}_z$

This condition gives the following equations

$$v\left(1\right)=cos\beta_0 \quad and \quad w\left(1\right)=sin\beta_0 \qquad (28)$$

Hyper stick condition: Micro rotation on the boundary is $l_\Gamma = \frac{1}{2} Curl Q_\Gamma$, where Γ represents boundary. This condition gives the following equations

$$B(1) = 0 \;\; and \;\; C(1) = \sigma_1 \tag{29}$$

As $\boldsymbol{q}$ and υ are at rest as $r \to \infty$ the solutions of (21) and (23) can be written as

$$\upsilon = a_1 K_1(\lambda_1 r) + a_2 K_1(\lambda_2 r) \tag{30}$$

$$B = a_3 K_1(\alpha_1 r) + a_4 K_1(\alpha_2 r) \tag{31}$$

Now the constants a_1,a_2,a_3 and a_4 can be found out numerically for different values of micropolar parameters by using the boundary conditions (28) and (29) in (25),(27),(30) and (31).

3 Calculation for drag

The drag D acting on a cylinder of length L is given by

$$D = aL \int_0^{2\pi} (T_{21} cos\beta_0 + T_{31} sin\beta_0) d\theta \tag{32}$$

The stress components in (32) are defined by the following constitutive equation for micropolar fluids [Eringen 1, 2]

$$T_{ij} = -p\delta_{ij} + (2\mu + \kappa) e_{ij} + \kappa\varepsilon_{ijm}(\omega_m - \upsilon_m) \tag{33}$$

where $\omega_m = \frac{1}{2}(\nabla_1 \times Q)_m$ the subscript m represents component in mth direction, e_{ij} is the strain rate tensor and ε_{ijm} is the alternative symbol. Now the stress components T_{31} and T_{21} on the cylinder (at r= 1) can be calculated as

$$\begin{aligned} T_{31} &= \frac{q_0(\mu+\kappa)}{as}\Big(a_3 K_1(\alpha_1)\left((1-c)\alpha_1^2 - cs\right) + a_4 K_1(\alpha_2) \times \\ &\quad \left((1-c)\alpha_2^2 - cs\right) - \frac{\alpha_1^2\alpha_2^2(1-c)}{iRe\sigma_2}\Big) e^{i\sigma_2 t} \end{aligned} \tag{34}$$

and

$$
\begin{aligned}
T_{21} \;=\; & \frac{q_0\left(\mu+\kappa\right)}{a}\left[a_1\left\{K_1\left(\lambda_1\right)\left(\frac{2\left(b_1+\lambda_1^2\right)iRe\sigma_1}{\lambda_1^2\lambda_2^2}-c\right)-\right.\right.\\
& \left.\lambda_1K_2\left(\lambda_1\right)\left(\frac{\left(b_1+\lambda_1^2\right)iRe\sigma_1}{\lambda_1^2\lambda_2^2}+1-c\right)\right\}+\\
& a_2\left\{K_1\left(\lambda_2\right)\left(\frac{2\left(b_1+\lambda_2^2\right)iRe\sigma_1}{\lambda_1^2\lambda_2^2}-c\right)-\right.\\
& \left.\left.\lambda_2K_2\left(\lambda_2\right)\left(\frac{\left(b_1+\lambda_2^2\right)iRe\sigma_1}{\lambda_1^2\lambda_2^2}+1-c\right)\right\}\right]e^{i\sigma_1 t}
\end{aligned}
\tag{35}
$$

Now finally the non–dimensional drag D' is given by

$$D' = \left(T_{21}cos\beta_0 + T_{31}sin\beta_0\right) \quad on \quad r=1 \tag{36}$$

where $D' = \dfrac{D}{2\pi L\mu q_0}$

4 Numerical calculation and results

The analytical expressions for the non-dimensional velocity components v, w and micro rotation components B, C and drag are given by (28), (29), (23), (25) and (34) respectively. For different values of the parameters like cross viscosity parameter or coupling number c, Reynolds number Re, couple stress parameter s and Gyration parameter ε on velocity components v, w and micro rotation components B, C are computed numerically and results are graphically presented in Figs1–20. The drag is calculated numerically at different times for fixed σ_1 and σ_2.

When the angle β_0=0 the problem reduces to rotatory oscillations about the axis of the cylinder. When $\beta_0 = \pi/2$, the problem becomes the special case of longitudinal oscillations along the axis of the cylinder. When $\sigma_1 = \sigma_2$ and oscillations are periodic, our results are in correlation with the results of Calmelet-Eluhu and Mazumdar [7].

The numerical results are presented in the form of graphs at s=10, c=0.4, ε=0.2, Re=0.7, σ_1=1.5, σ_2=2.5, β_0=0.7, $t = \pi$. It can be seen from Figs 2–5 that as the Cross viscosity parameter c increases the axial velocity w and micro rotation C are decreasing whereas transverse velocity v and micro rotation B are increasing near to cylinder up to double the distance of radius of the cylinder then are decreasing as distance increases.

It can be seen from Figs 6–9 that as the Gyration parameter ε has no effect on the velocities v, w and micro rotation components B, C. i.e., the variation in the values of ε does not result in much variation in the values of v, w, B and C.

It can be seen from Figs 10–13 that as the Reynolds number Re increases the velocities v, w and micro rotation C are decreasing and the maximum values of micro rotation B are increasing.

From figs 14–17, we observe that as couple stress parameter s increases the transverse velocity v and micro rotation C are decreases whereas maximum values of micro rotation B increase, but the effect on w is insignificant.

The non-dimensional drag is calculated numerically for different values of non-dimensional time in multiples of π/σ_2 at fixed values of σ_1, σ_2 and the results are shown in the Fig 18. It can be seen from fig 18 that as c increases the amplitude of drag decreases.

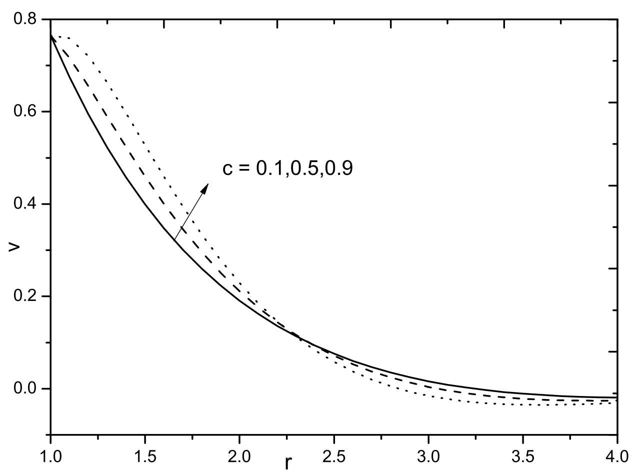

Figure 2: variation of v with r

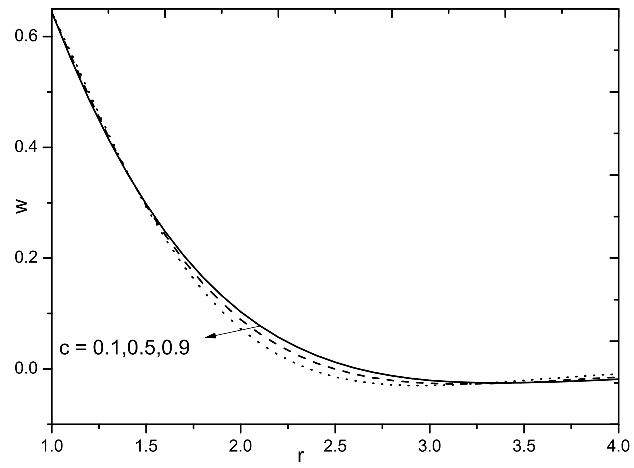

Figure 3: variation of w with r

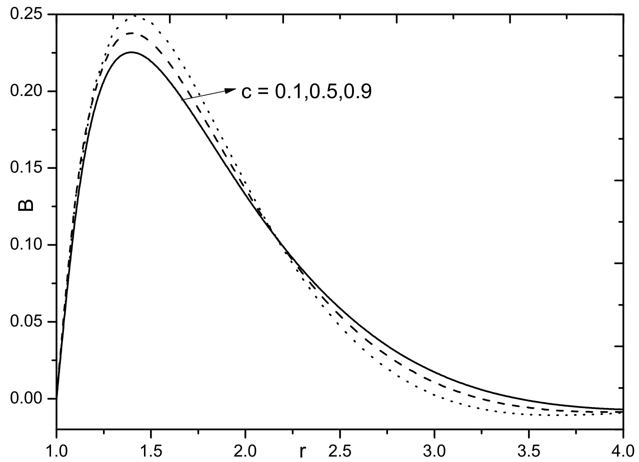

Figure 4: variation of B with r

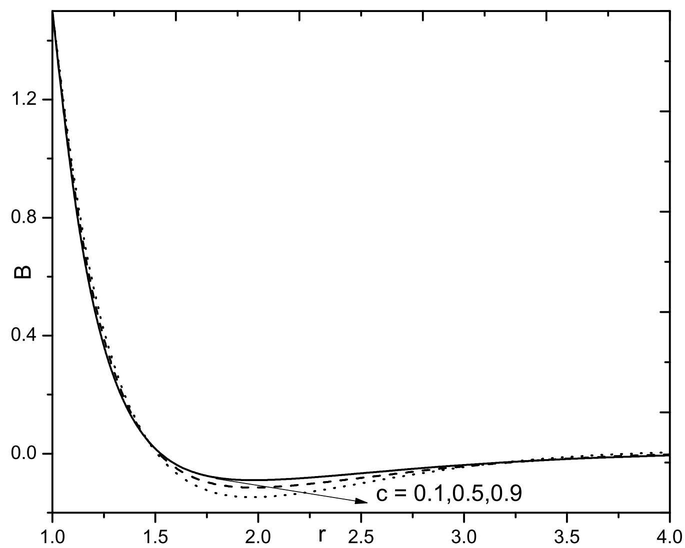

Figure 5: variation of C with r

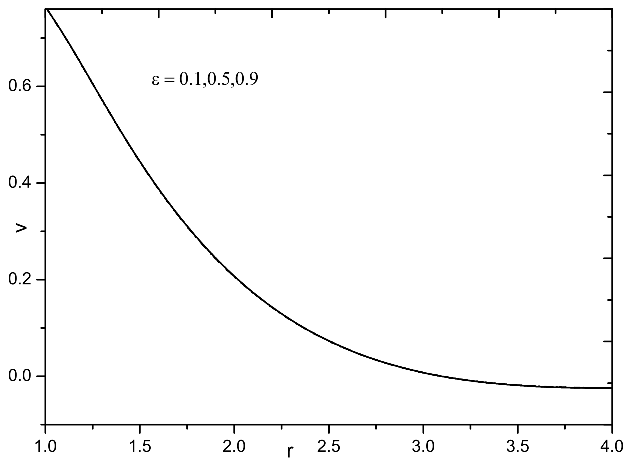

Figure 6: variation of v with r

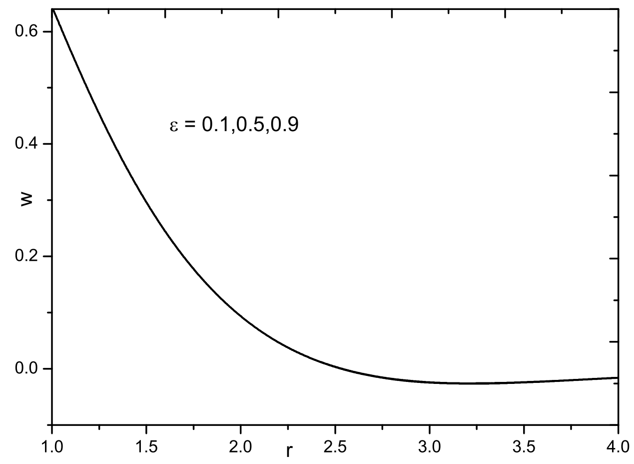

Figure 7: variation of w with r

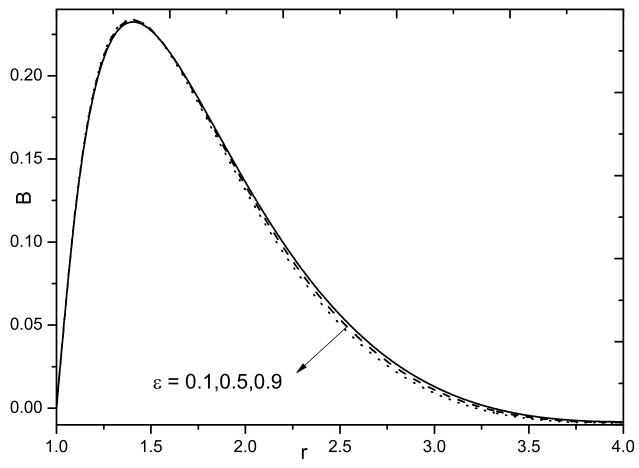

Figure 8: variation of B with r

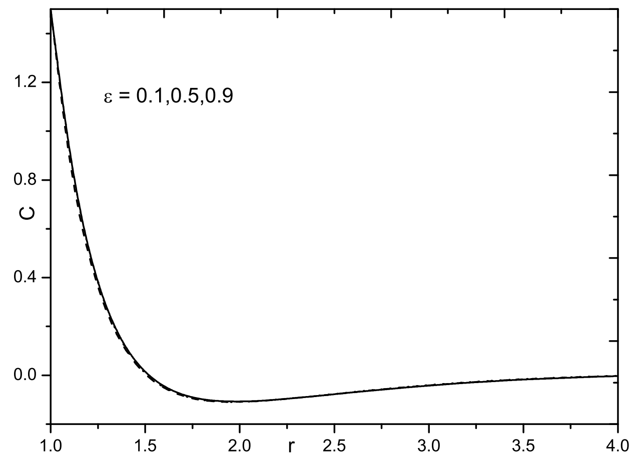

Figure 9: variation of C with r

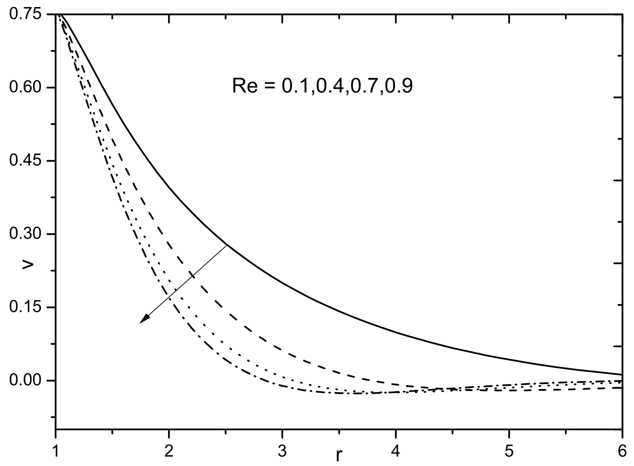

Figure 10: variation of v with r

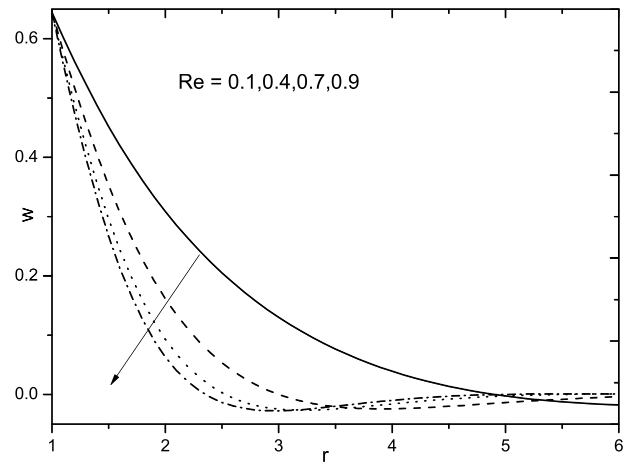

Figure 11: variation of w with r

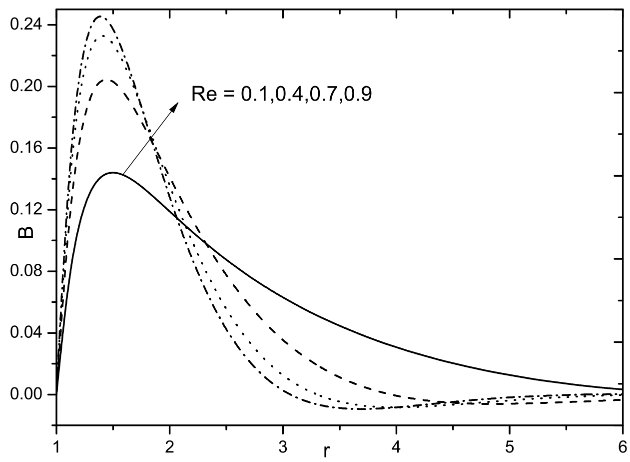

Figure 12: variation of B with r

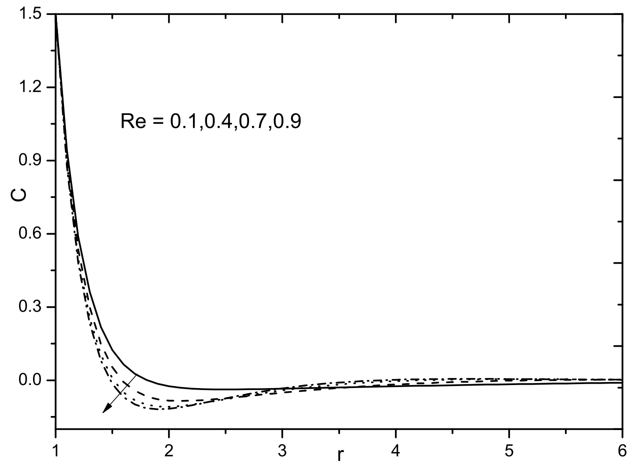

Figure 13: variation of C with r

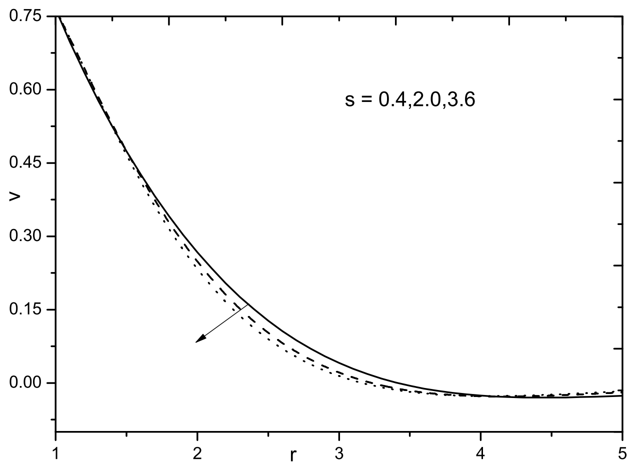

Figure 14: variation of v with r

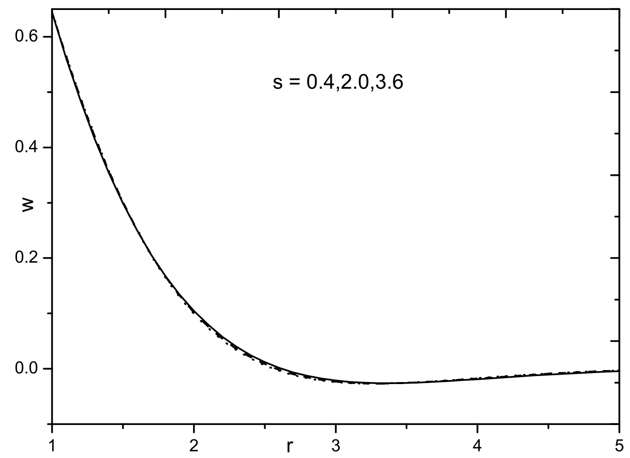

Figure 15: variation of w with r

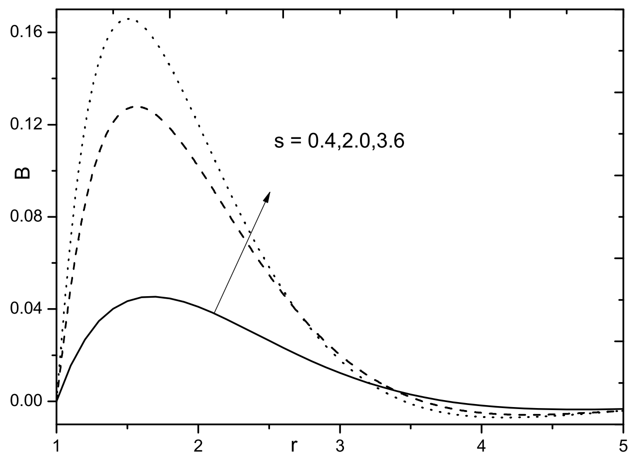

Figure 16: variation of B with r

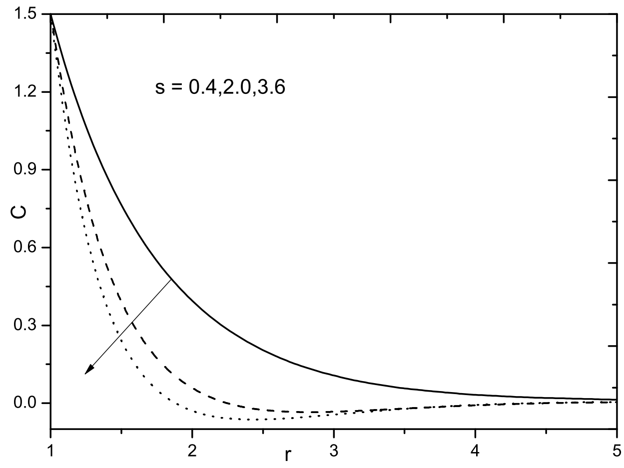

Figure 17: variation of C with r

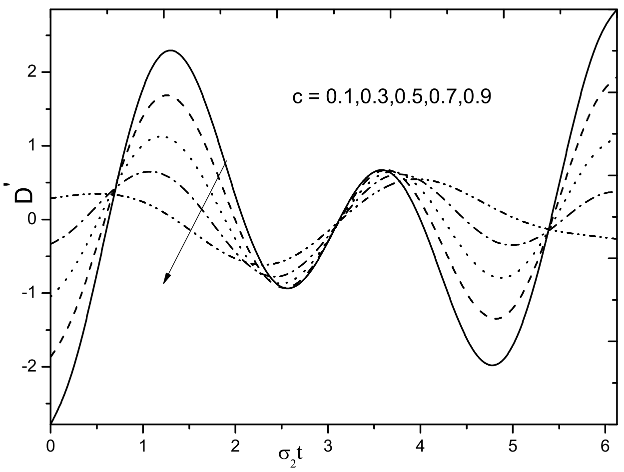

Figure 18: variation of D' with $\sigma_2 t$

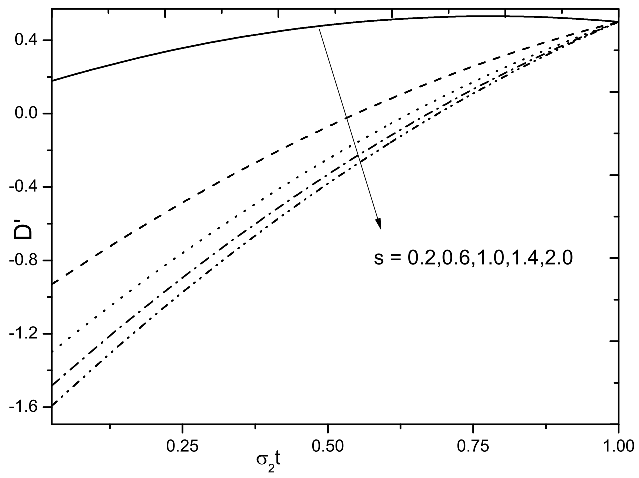

Figure 19: variation of D' with c

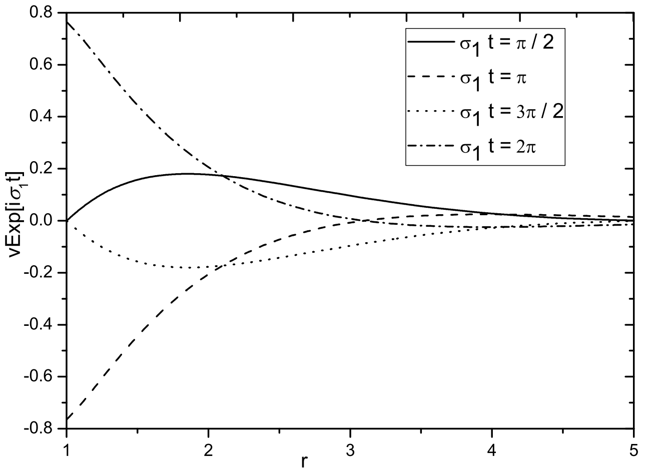

Figure 20: variation of $v\mathrm{Exp}(\mathrm{i}\sigma_1\mathrm{t})$ with r

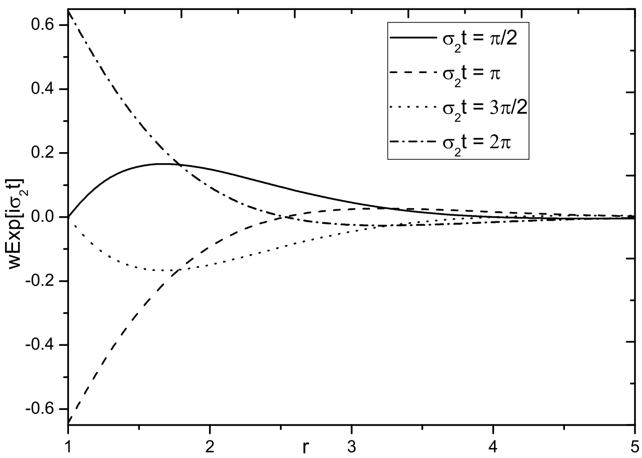

Figure 21: variation of wExp(iσ_2t) with r

In fig 19, it is observed that as s increases, the amplitude of oscillation for the drag decreases and all the curves are assuming the same shape nearly after s exceeds a certain value. Drag in the case of viscous fluids is less than that of the micropolar fluids.

We get the case of viscous fluids from the micropolar fluid by applying the limit $c \to 0$ and $s \to \infty$. These results are shown in Figs.20–21 for velocities v and w and our results are in good agreement with the observations of Ramkissoon [6] in the case of viscous fluids.

References

[1] A.C.Eringen, Theory of micropolar fluids, J. Math. Mech, 16, 1–18, (1966).

[2] A.C.Eringen, Theory of thermo-microstretch fluids and bubbly liquids, Int. J. Eng. Sci. 28, 133– 143, (1990).

[3] Stokes G.G. (1886): On the effect of rotation of cylinders and spheres about their own axes in increasing the logarithmic decrement of the arc of vibration.(Mathematical and Philosophical Paper-5) Cambridge: Cambridge University Press, England, pp 207–214.

[4] Casarella M. J and Laura P.A (1969): Drag on oscillating rod with longitudinal and torsional motion, J. Hydronaut., Vol 3, pp 180–183.

[5] Rajagopal K.R (1983): Longitudinal and Torsional oscillation of a rod in a non-Newtonian fluid, Acta. Mech., Vol 49, pp 281–285.

[6] Ramkissoon H and Majumdar S.R (1990): Flow due to the longitudinal and torsinal oscillations of a cylinder, ZAMP, Vol 41, pp 598–603.

[7] Calmelet-Eluhu C and Mazumdar D R (1998): Flow of Micropolar fluid through a circular cylinder subject to longitudinal and torsinal oscillations. Mathl. Comput. Modelling, Vol 27, pp 69–78.

[8] Owen.D and Rahaman K (2006): On the flow of an Oldroyd-B liquid through a straight circular tube performing longitudinal and torsinal oscillations of different frequencies, Mathematica, Vol 14, pp 1–9.

[9] Calmelet-Eluhu C and Rosenhaus V (2001): Symmetries and solutions of a micropolar through a cylinder. Acta. Mech., Vol 147, pp 59–72.

[10] Ramkissoon H, Easwaran. C.V and Majumdar S.R (1991): Longitudinal and Torsional oscillation of a rod in a polar fluid, Int. J. Engng. Sci, Vol 29(2), pp 215–221.

[11] Bandelli R , Lapczyk I and Li H (1994): Longitudinal and torsional oscillations of a rod in a third grade fluid, Int. J. Non-linear Mech, Vol 29, pp 397–408.

[12] Rajagopal K. R and Bhatnagar R. K (1995): Exact solutions for some simple flows of an Oldroyd–B fluid, Acta. Mech, Vol 113, pp 233–239.

[13] Pontrelli, G (1997): Longitudinal and torsional oscillations of a rod in an Oldroyd-B fluid with suction or injection, Acta Mech., Vol 123, pp 57–68.

[14] Akyildiz.F.T (1998): Longitudinal and torsinal oscillations of a rod in a viscoelastic fluid, Rheol. Acta, Vol 37, pp 508–511.

[15] Fetecau. C and Corina Fetecau (2006): Starting solutions for the motion of a second grade fluid due to longitudinal and torsional oscillations of a circular cylinder, Int. J. Engng. Sci, Vol 44, pp 788–796.

[16] Vieru D, Akhtar W, Fetecau C and Corina Fetecau (2007): Starting solutions for the oscillating motions of a Maxwell fluid in cylindrical domain, Meccanica, Vol 42, pp 573–583.

[17] Laura Bridglal and Karim Rahaman (2008): Upper convected Maxwell fluid due to solid rod oscillating with different frequencies. J. Engng. & Appl. Sci, Vol 3, pp 651–655.

[18] Mehrdad Massoudi and Tran X.Phouc (2008): On the motion of a second grade fluid due to longitudinal and torsinal oscillations of a cylinder-A numerical study. Appl. Math. Comput. Vol 203, pp 471–481.

Submitted in January 2013, revised in October 2013, accepted in March 2014

Nestabilno tečenje mikropolarne tečnosti izazvano uzduzv znim i torzionim oscilacijama kružnog cilindra

Proučava se tečenje mikropolarne tečnosti u beskrajnom prostoru koje je izazvano uzdužnim i torzionim oscilacijama kružnog cilindra Analitički izrazi za komponente brzine i mikro obrtanja su dobijeni korišćenjem odsustva klizanja kao i uslova hiper-prilepljivanja na granici. Posledice broja spregnutosti, Rejnoldsovog broja i žiro-parametra na poprečne i uzdužne komponente brzine su prikazane i slikovito objašnjene. Takodje, eksplicitni izraz za silu otpora na zidu cilindra je izveden i učinci relevantnih parametara na otpor su grafički prikazani.

doi:10.2298/TAM1401001N Math. Subj. Class.: 74A35; 74A60; 76A99.